PCCP

COMMUNICATION

View Article Online
View Journal | View Issue

Cite this: *Phys. Chem. Chem. Phys.*, 2016, **18**, 31997

Received 6th September 2016,
Accepted 24th October 2016

DOI: 10.1039/c6cp06155a

www.rsc.org/pccp

Effect of the meniscus contact angle during early regimes of spontaneous imbibition in nanochannels

Nabin Kumar Karna,[ab] Elton Oyarzua,[a] Jens H. Walther[cd] and Harvey A. Zambrano*[a]

Nanoscale capillarity has been extensively investigated; nevertheless, many fundamental questions remain open. In spontaneous imbibition, the classical Lucas–Washburn equation predicts a singularity as the fluid enters the channel consisting of an anomalous infinite velocity of the capillary meniscus. Bosanquet's equation overcomes this problem by taking into account fluid inertia predicting an initial imbibition regime with constant velocity. Nevertheless, the initial constant velocity as predicted by Bosanquet's equation is much greater than those observed experimentally. In the present study, large scale atomistic simulations are conducted to investigate capillary imbibition of water in slit silica nanochannels with heights between 4 and 18 nm. We find that the meniscus contact angle remains constant during the inertial regime and its value depends on the height of the channel. We also find that the meniscus velocity computed at the channel entrance is related to the particular value of the meniscus contact angle. Moreover, during the subsequent visco-inertial regime, as the influence of viscosity increases, the meniscus contact angle is found to be time dependent for all the channels under study. Furthermore, we propose an expression for the time evolution of the dynamic contact angle in nanochannels which, when incorporated into Bosanquet's equation, satisfactorily explains the initial capillary rise.

Advances in micro- and nano-fabrication techniques provide the ability to develop a variety of structures with well-defined features. Promissory integration of micro- and nanofluidic structures into complex nanofluidic systems such as nano-Lab On a Chip (LOC) and nanosensor devices requires a comprehensive understanding of the driving mechanisms for fluid transport in nanoconfinement. Due to the large surface to volume ratio inherent to nanofluidics, the influence of surface effects and interfacial liquid dynamics presents fundamental challenges to the application of macroscopic theories of capillary flow in nanoconfinement. Indeed, in the topic of capillarity, the classical Lucas–Washburn (LW) equation,[1] which is derived assuming a single force balance between viscous friction and capillary pressure, has proved adequate for describing the uptake of viscous fluids in relatively large capillaries and porous solid materials.[2] Nevertheless, the LW equation fails to describe the initial stage of liquid penetration.[3–5] The main drawback of the LW equation is the prediction of a singularity at the liquid uptake, which has been attributed to not taking inertia into consideration.[6–9]

Bosanquet's equation, which is equivalent to Washburn's equation for long filling times,[10] describes the imbibition kinetics taking the inertia effect into account, thus overcoming the singularity present in the LW equation. Recently, it has been shown that the imbibition kinetics are divided into three main flow regimes:[3,5] an initial stage, the inertial or inviscid regime, where the capillary force is balanced only by the inertial drag and characterized by a plug flow velocity profile; thereafter, a regime in which the force balance has contributions from both inertia and viscous friction; and subsequently, a regime wherein viscous forces dominate the capillary force balance.[2,3,5]

It is noteworthy that during the inviscid flow regime, the Bosanquet solution predicts a constant velocity;[2–5] therefore, in a non-accelerating imbibing fluid the capillary force must be exactly balanced by fluid inertia. It seems to be contradictory to the usually assumed immediate and continuous variation of the meniscus contact angle right from the channel entrance[11–13] as the continuously increasing capillary force due to Laplace pressure cannot exactly balance the inertial force induced by the fluid inertia.[2,4,5,10,14] Therefore, it implies that all the other factors during the capillary imbibition remained constant, and there should exist a meniscus with a constant contact angle during the inertial regime. Furthermore, it has been found that the initial constant velocity is lower than that predicted by Bosanquet's equation.[2,5,14,15]

In this study, we address this problem by performing large scale molecular dynamics simulations of the initial imbibition

[a] *Universidad de Concepcion, Concepcion, Chile. E-mail: harveyzambrano@udec.cl; Fax: +56 41224 7491; Tel: +56 41266 1468*
[b] *Unidad de Desarrollo Tecnologico, Coronel, Chile*
[c] *Technical University of Denmark, Copenhagen, Denmark*
[d] *Chair of Computational Science, ETH Zurich, Zurich, Switzerland*

of nano-confined water into silica channels. We report the time evolution of the capillary front and meniscus contact angle during the capillary filling of nanochannels with heights ranging from 4 to 18 nm. Providing an atomistic description of the capillary filling process in its earliest time stage and during the subsequent transition towards a fully developed flow regime, our study allows complete characterization of the kinetics of liquid imbibition in nanochannels, which explains the initial meniscus formation and its relationship to the constant velocity during the inertial regime.

Bosanquet's equation

Bosanquet's solution of capillary imbibition for an infinite rectangular capillary takes the form of eqn (1)[5]:

$$l(t)^2 = \frac{2A_I^2}{B}\left[t - \frac{1}{B}(1 - \exp(-Bt))\right] \quad (1)$$

A_I and B in the above equation are given by

$$A_I = \sqrt{\left(\frac{2\gamma\cos\theta}{\rho H}\right)} \quad (2)$$

$$B = \frac{12\mu}{\rho H^2} \quad (3)$$

where A_I corresponds to the initial velocity just at the entrance. The equilibrium contact angle in this equation is assumed to be attained instantaneously, which is contrary to more recent studies.[7,16–21] Hence, it is important to account for the dynamic contact angle (DCA) in Bosanquet's equation to adequately explain the capillary rise. We propose that DCA, which can only be seen after the inertial regime, can be modeled by eqn (4):

$$\cos\theta_d = \begin{cases} \cos\theta_i & \text{for } t \le t_i \\ \cos\theta_e\left(1 - \exp\left(-\frac{t}{\tau}\right)\right) & \text{for } t > t_i \end{cases} \quad (4)$$

In the above equation, τ should be proportional to characteristic time for fully developed flow and is given by eqn (5),[22] and t_i refers to the time during which the inertial regime persists and θ_i is the initial contact angle made by the liquid with the nanocapillary walls.

$$\tau = K_1\left(\frac{H^2\rho}{\mu}\right) \quad (5)$$

We consider this correlation after the inertial regime as viscous force starts playing a significant role and inertia becomes negligible.

Inertial regime

The inertial regime refers to the "inviscid regime" and is characterized by constant velocity (U_o), where the filling is driven by a balance between the inertial force and capillary forces, which results in

$$U_o \sim \sqrt{\left(\frac{\gamma}{\rho H}\right)} \quad (6)$$

Assuming $l \sim H$, during the inertial regime and taking into account $U_o = l/t_i$, we obtain

$$t_i = K_2\sqrt{\left(\frac{H^3\rho}{\gamma}\right)} \quad (7)$$

where K_2 is the proportionality constant. To study the validity of these models we conduct a series of MD simulations using the MD package FASTTUBE[5,23–26] to investigate the initial imbibition in silica nanochannels. The potential parameters used in the present study have been calibrated in our previous study[26] wherein the silica–water interaction potential was calibrated using as a criterion the water contact angle reported by Thamdrup *et al.*[27] Water is described using a modified version[28] of the simple point charge SPC/E model[29] and silica by the TTAMm model developed by Guissani and Guillot.[30] For further details of the potentials used, we refer the reader to Zambrano *et al.*[26] and Oyarzua *et al.*[5]

Rectangular nanochannels of different heights (4, 6, 10, 14 and 18 nm) were built using amorphous silica slabs (Fig. 1). For details of slab construction, the readers are requested to refer to our previous study.[5] In the simulations, using a time step of 2 fs, a water slab is coupled to a Berendsen heat bath[5] at 300 K during 0.5 ns; then, the thermostat is disconnected and the simulations are conducted in the microcanonical ensemble (*NVE*) until the system is equilibrated. Subsequently, the water slab is released from the rest to move spontaneously towards the silica channels. The number of water molecules in each simulation is listed in Table 1.

The initial velocity and the inertial time (t_i) for each simulation were estimated from the atomic trajectories. Subsequently, the value of τ was approximated such that the dynamic contact angles predicted using eqn (4) fitted those obtained using the simulation results. Then, the values of K_2, as indicated in eqn (7), were calculated using the values of t_i estimated from the simulation results. Similarly, the contact angle at time t_i was obtained and the velocity in the inertial regime was calculated for each channel using eqn (3). The instantaneous position of the advancing capillary front is tracked along the direction perpendicular to the flow of water to find the penetration length of water. An example of the meniscus is shown in Fig. 1. In Fig. 2, we plot the temporal evolution of the imbibition length as a function of time for all the channels under study. The time evolution of penetration lengths during early time periods, as displayed in the figures, is linear, which indicates a capillary flow with constant velocity, thus confirming the existence of the inertial regime as predicted by Bosanquet.[2,5,10] It can be observed that the inertial regime is

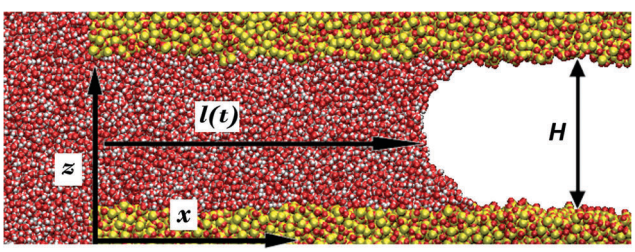

Fig. 1 A snapshot of the capillary filling for a 6 nm silica nanochannel.

Table 1 Configurational details of water imbibition in silica nanochannels

Case no.	H (nm)	No. of H_2O molecules
1	4	18 000
2	6	22 000
3	10	32 000
4	14	52 000
5	18	56 000

H = channel height; channel length was kept constant (31.6 nm) in all the cases.

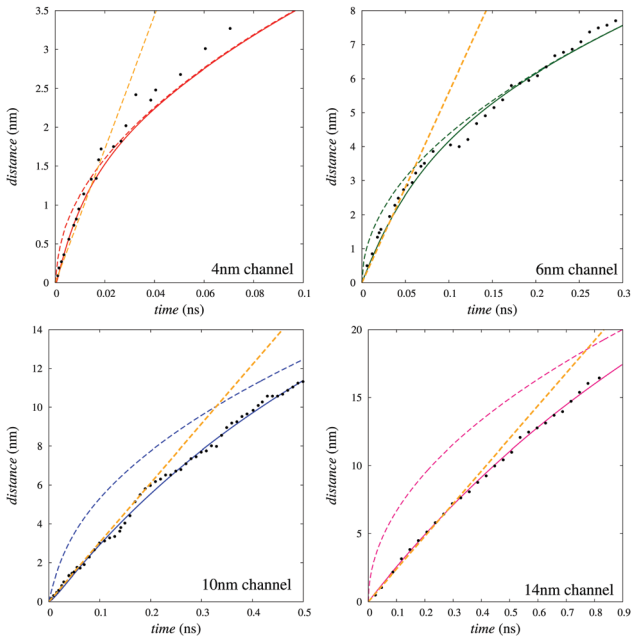

Fig. 2 Nanocapillary imbibition length as a function of time for different height of capillaries. The black dots represent the imbibition length as a function of time. The straight yellow dashed lines are visual guides to indicate the $l(t) = A_l t$, which also illustrate estimated times of inertial regime. The solid lines depict the fits of modified Bosanquet's equation to the experimental data. The colored dotted lines are visual guide lines to indicate the original Bosanquet's equation.

more prominent in a channel of greater height. Inertial times for all the cases were directly calculated from the simulation data. The slope of the plot of inertial time against $\sqrt{H^3\rho/\gamma}$, gives an estimated value of K_2, mentioned in eqn (7), and is approximately found to be 1 (Fig. 4). Hence, the inertial time is given by eqn (8):

$$t_i = \sqrt{\left(\frac{H^3\rho}{\gamma}\right)} \quad (8)$$

As mentioned earlier, the velocity during the inertial regime remains constant (Fig. 2), which implies that the dynamic contact angle observed during this regime remains constant (Fig. 3), which is consistent with the hydrodynamic models of contact angle development,[17,21,31] which relates DCA to the capillary number and constant velocity during the inertial regime predicted by Bosanquet's equation.[10] In other words, the DCA remains constant during the inertial regime when the

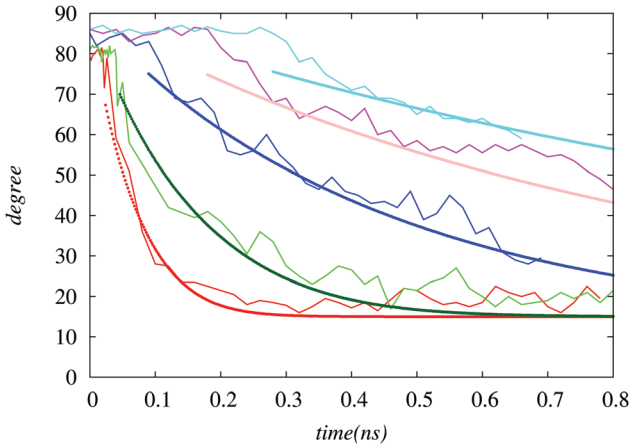

Fig. 3 Measured contact angles (dotted lines) and those predicted by the model (solid lines) during the nanocapillary imbibition in silica nanochannels of different heights. The red, green, blue, pink and cyan lines represent the contact angles for 4, 6, 10, 14 and 18 nm channels, respectively.

Table 2 Values of the important parameters during initial rise

H (nm)	E. vel (nm ns^{-1})	C. vel (nm ns^{-1})	t_i (ns)	τ (ns)
4	76	77.5	0.025	0.047
6	56	54	0.047	0.105
10	33	35	0.11	0.29
14	23	25	0.19	0.57
18	18	20	0.28	0.95

H = channel height, E. vel = estimated velocity, C. vel = calculated velocity, t_i = inertial time, τ = adjusting parameter for DCA.

velocity is constant and gradually decreases with decreasing velocity when viscous losses in the bulk become significant till it apparently attains the equilibrium value. A constant contact angle during the inertial regimes implies that this angle should be achieved right at the channel entrance when the liquid comes into contact with the upper and lower solid walls. For a channel with constant height, the imbibition velocity depends only on the contact angle made by fluid with the walls.[6] As it is well known that the initial velocity decreases with channel height,[5] as seen in Table 2, the contact angle which determines the velocity during the inertial regime[6] should increase with channel height. This has been confirmed in the present study and can be seen in Fig. 3. It leads to an interesting conclusion that the initial angle made by water at the channel entrance is different from 90° and depends on the height and material of the channel.[32] It also concludes that during inertial filling capillary force is balanced by inertial force as predicted by Bosanquet. It is noteworthy that the product of the cosine of the initial contact angle made by the fluid with the nanochannel walls and the height of the channel remains constant and is given by

$$H\cos\theta_i = C \quad (9)$$

where C is a constant and most probably depends on the materials in the system and the pre-imbibition conditions.[2,33] For the silica water system, this constant is approximately equal to 0.67 (Fig. 4). This also explains the low velocity observed

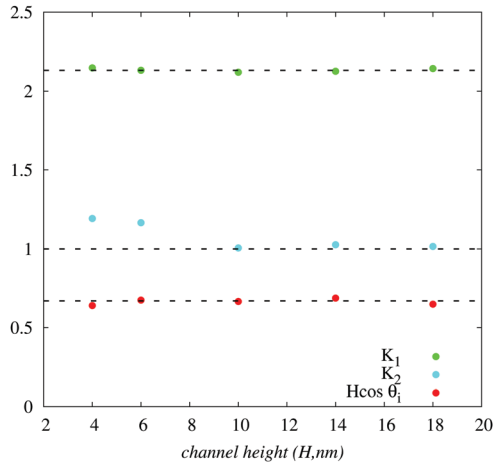

Fig. 4 Calculated values of the constants as a function of channel height (H). The dotted lines represent linear fits, while the coloured dots are the measured values.

during the capillary filling which cannot be explained using original Bosanquet's equation. Hence, we propose that effective Bosanquet's velocity is given by eqn (10):

$$A = \sqrt{\left(\frac{2\gamma \cos\theta_i}{\rho H}\right)} \tag{10}$$

where θ_i is the initial contact angle made by the liquid surface with the nanochannel walls. The above equation satisfactorily explains the observed and predicted velocities during the inertial regime, as can be seen in Table 2. The initial constant angle determined using eqn (9) remains constant for time t_i, which can be predicted using eqn (8), after which the dynamic contact angle is observed and is described using eqn (4). The values of τ mentioned in this equation can be estimated using eqn (11), substituting the average value of K_1 from Table 2.

$$\tau = 2.132\left(\frac{H^2\rho}{\mu}\right) \tag{11}$$

Similar results have been observed by Fries[3] for cylindrical channels when the capillary filling is determined by the balance between the viscous and capillary forces. This time (t_f) as determined by Fries[3] is given by

$$t_f = 2.1151\left(\frac{H^2\rho}{\mu}\right) \tag{12}$$

The constant angle observed during the inertial regime and good approximation of initial velocity obtained from the simulations and those calculated using modified Bosanquet's equation confirm that the predominant forces during the inertial regime are inertial and capillary forces and other forces are not relevant during the initial filling, contrary to the predictions made by other researchers.[34–36] It can be observed that Bosanquet's equation modified by including a dynamic contact angle satisfactorily describes the initial regimes of capillary imbibition (Fig. 2).

In summary, the present study revealed that the velocity and contact angle remain constant during the initial time of nanocapillary imbibition, thus confirming the predictions by Bosanquet that the predominant forces during the inertial regime are inertial and capillary forces. We find that the dynamic contact angle is observed after the inertial regime when viscous dissipation becomes more prominent. The dynamic contact angle is found to be height and time dependent for the channels under study. The incorporation of the proposed time dependent relationship for DCA in Bosanquet's equation successfully predicts the initial filling kinetics of the silica–water system as well as the initial velocity at the entrance. Initial contact angles different from 90° have been observed for all the channels, which establishes that, for a given system, the initial contact angle depends on the height of the channel.

Acknowledgements

This research was funded by CONICYT under FONDECYT project no. 11130559 and under CONICYT scholarship no. 0001156 and no. 21140427. We also thank the partial financial support from the University of Concepcion under VRID project no. 21496651. The authors thank computational support from the Danish Center for Scientific Computing (DCSC) and from the National Laboratory for High Performance Computing Chile (NLHPC). Furthermore, the authors wish to acknowledge Enrique Wagemann for valuable scientific discussions.

References

1 E. W. Washburn, *Phys. Rev.*, 1921, **17**, 273–283.
2 K. G. Kornev and A. V. Neimark, *J. Colloid Interface Sci.*, 2001, **235**, 101–113.
3 N. Fries and M. Dreyer, *J. Colloid Interface Sci.*, 2008, **327**, 125–128.
4 S. Das, P. R. Waghmare and S. K. Mitra, *Phys. Rev. E: Stat., Nonlinear, Soft Matter Phys.*, 2012, **86**, 067301.
5 E. Oyarzua, J. H. Walther, A. Mejia and H. A. Zambrano, *Phys. Chem. Chem. Phys.*, 2015, **17**, 14731–14739.
6 D. Quere, E. Raphael and J.-Y. Ollitrault, *Europhys. Lett.*, 1999, **15**, 3679–3682.
7 A. Siebold, M. Nardin, J. Schultz, A. Walliser and M. Oppliger, *Colloids Surf., A*, 2000, **161**, 81–87.
8 D. Quere, *Europhys. Lett.*, 1997, **39**, 533–538.
9 E. J. LeGrand and W. A. Rense, *J. Appl. Phys.*, 1945, **16**, 843–846.
10 C. H. Bosanquet, *Phil. Mag. Ser. 6*, 1923, **45**, 525–531.
11 G. Martic, F. Gentner, D. Seveno, D. Coulon, J. De Coninck and T. D. Blake, *Langmuir*, 2002, **18**, 7971–7976.
12 G. Martic, T. D. Blake and J. D. Coninck, *Adv. Colloid Interface Sci.*, 2005, **21**, 11201–11207.
13 W. Stoberg, *J. Am. Chem. Soc.*, 2012, **28**, 14488–14495.
14 C. J. Ridgway, P. A. C. Gane and J. Schoelkopf, *J. Colloid Interface Sci.*, 2002, **252**, 373–382.
15 F. Chauvet, S. Geoffroy, A. Hamoumi, M. Prat and P. Joseph, *Soft Matter*, 2012, **8**, 10738.
16 D. Duvivier, T. D. Blake and J. De Coninck, *Langmuir*, 2013, **29**, 10132.

17 R. G. Cox, *J. Fluid Mech.*, 1998, **357**, 249–278.
18 E. B. Dussan, *Annu. Rev. Fluid Mech.*, 1979, **11**, 371–400.
19 J. E. Seebergh and J. C. Berg, *Chem. Eng. Sci.*, 1992, **47**, 4455–4464.
20 M. Bracke, F. De Voeght and P. Joos, The kinetics of wetting: the dynamic contact angle, *Trends in Colloid and Interface Science III*, Steinkopff, 1989, vol. 136, pp. 142–149.
21 T. Jiang, O. Soo-Gun and J. C. Slattery, *J. Colloid Interface Sci.*, 1979, **69**, 74–77.
22 G. L. Batten, *J. Colloid Interface Sci.*, 1984, **102**, 513–518.
23 J. H. Walther, T. Werder, R. L. Jaffe and P. Koumoutsakos, *Phys. Rev. E: Stat., Nonlinear, Soft Matter Phys.*, 2004, **69**, 062201.
24 T. Werder, J. H. Walther, R. Jaffe, T. Halicioglu, F. Noca and P. Koumoutsakos, *Nano Lett.*, 2001, **1**, 697–702.
25 H. A. Zambrano, J. H. Walther, P. Koumoutsakos and I. F. Sbalzarini, *Nano Lett.*, 2009, **9**, 66–71.
26 H. A. Zambrano, J. H. Walther and R. L. Jaffe, *J. Mol. Liq.*, 2014, **198**, 107–113.
27 L. H. Thamdrup, F. Persson, H. Bruus, A. Kristensen and H. Flyvbjerg, *Appl. Phys. Lett.*, 2007, **91**, 163505.
28 M. Levitt, M. Hirshberg, K. E. Laidig and V. Daggett, *J. Phys. Chem. B*, 1997, **101**, 5051–5061.
29 H. J. C. Berendsen, J. R. Grigera and T. P. Straatsma, *J. Phys. Chem.*, 1987, **91**, 6269–6271.
30 Y. Guissani and B. Guillot, *J. Chem. Phys.*, 1996, **104**, 7633–7644.
31 O. V. Voinov, *Fluid Dyn.*, 1976, **11**, 714–721.
32 A. Lukyanov and Y. Shikhmurzaev, *Phys. Rev.*, 2007, **75**, 1539–3755.
33 J. Szekely, A. W. Neumann and Y. K. Chuang, *J. Colloid Interface Sci.*, 1971, **35**, 273–278.
34 T. Andrukh, D. Monaenkova, B. Rubin, W.-K. Lee and K. G. Kornev, *Soft Matter*, 2014, **10**, 609–615.
35 B. Zhmud, F. Tiberg and K. Hallstensson, *J. Colloid Interface Sci.*, 2000, **228**, 263–269.
36 A. Hamraoui, K. Thuresson, T. Nylander and V. Yaminsky, *J. Colloid Interface Sci.*, 2000, **226**, 199–204.